

Green synthesis of silver nanoparticles using banana flower extract, and their antibacterial activity

Weiming, G., Quanfeng, H., Jianxia S., *Dan, L. and Xuejuan, D.

Faculty of Chemical Engineering and Light Industry, Guangdong University of Technology,
Guangzhou 510006, People's Republic of China

Article history

Received:

21 May 2022

Received in revised form:

31 July 2022

Accepted:

22 November 2022

Keywords

banana flower extract,
silver nanoparticles,
biosynthesis,
food-borne bacterial,
antibacterial activity

Abstract

Silver nanoparticles (AgNPs) were synthesised using banana flower extract (BFE) as a reducing and stabilising agent. Spherical, well-dispersed, and stable AgNPs were formed and characterised by ultraviolet-visible spectroscopy (UV-vis), transmission electron microscopy (TEM), X-ray diffraction (XRD), Fourier-transform infrared spectroscopy (FT-IR), thermal gravimetric analysis (TGA), and zeta potential. The *in vitro* antimicrobial properties of AgNPs against *Staphylococcus aureus* and *Escherichia coli* were then investigated. The minimum inhibitory concentration (MIC) of AgNPs against *S. aureus* and *E. coli* were 32 and 16 µg/mL, respectively. *E. coli* was more sensitive to AgNPs than *S. aureus* due to differences in cell wall structures of the bacteria. Regarding the bactericidal mechanisms of AgNPs, an increase in cell permeability and a distinctive deformation in cellular morphology was observed. The antibacterial effect decreased with the addition of the antioxidant N-acetyl-L-cysteine (NAC) which acted as ROS scavenger. In summary, the antibacterial mechanism was likely a combination of cell membrane damage and ROS induction.

DOI

<https://doi.org/10.47836/ifrj.30.3.06>

© All Rights Reserved

Introduction

Foodborne diseases are a widespread and growing public health and economic problem. Many outbreaks of pathogenic diseases are closely related to microbial contamination. The traditional antibacterial agents tend to lose their effectiveness over time due to increasing bacterial resistance. Advances in nanotechnology have opened new avenues for microbial control (Liu *et al.*, 2019), one of which is the synthesis of antimicrobial nanoparticles as a means of pathogenic inactivation (Guo *et al.*, 2020).

Silver nanoparticles (AgNPs) are attracting much interest because of their potent antibacterial activity to combat a wide range of bacterial pathogens (Küp *et al.*, 2020). AgNPs have several advantages for antibacterial treatments including a high surface area to volume ratio, amenability to surface modification, small size, and inert nature (El-Kheshen and El-Rab, 2012). As compared to classic antibiotics, the mode of bacteriostatic/bactericidal

action of AgNPs may not be against a specific molecular target, thus resulting in a reduced risk of bacterial resistance development. Rather, the potent antibacterial properties of AgNPs seem to reflect several mechanisms by which nanoparticles interact with microorganisms. These mechanisms involve the cell membrane surface, penetration, internal migration, and ROS generation induced by the ions leached from AgNPs (Joshi *et al.*, 2020). Acting together, these effects lead to bacterial cell death. The nature of AgNPs, their concentration, their size, and their shape are known to affect their antibacterial activity (Osonga *et al.*, 2020). Different approaches for the synthesis of AgNPs lead to their particular structure which in turn affects its antibacterial effect and modes of interactions with bacterial surfaces.

Methods for synthesising AgNPs can be divided into physical, chemical, and biological methods. Physical methods produce AgNPs of high quality but require special equipment and incur significant production costs (Arce *et al.*, 2017). The chemical synthetic methods are limited due to the use

*Corresponding author.

Email: dana0816@163.com

of toxic and highly reactive reagents that pose risks to the environment and to human health. The bioreduction method based on the use of microorganisms or plants is a very attractive approach with the advantages of environmental friendliness and low cost (Soto *et al.*, 2019; Nguyen *et al.*, 2020). When compared with the cumbersome screening and culture process of the microbial method, employing plant extraction is a simpler, cheaper, and more suitable route for the synthesis of stable AgNPs with controlled size and shape (Salayová *et al.*, 2021). A variety of plant and fruit extract sources such as leaf, root, latex, seed, and stem are being used for AgNPs synthesis (Arya *et al.*, 2018; Devanesan and AlSalhi, 2021; Padalia and Chanda, 2021). The key to some of these syntheses are believed to be polyphenols, acting as reducing agents which transfer a negative charge to Ag⁺ to form Ag atoms that subsequently further nucleate and condense to form larger AgNPs. The excess of negatively charged reducing agent adsorbed on the surface of the formed particles achieves electrostatic stabilisation at controllable sizes of the AgNPs (Rajeshkumar and Bharath, 2017).

Agricultural by-products are typically discarded. Recently, there has been a shift in the management of these by-products to converting them into value-added products. Since banana is an important crop worldwide, plantations produce tonnes of banana by-products each harvest season including peel, leaves, pseudostem, stalk, and stem (Padam *et al.*, 2014). Many scientific investigations on banana by-products especially on banana peels have been carried out (Lau *et al.*, 2020; Hikal *et al.*, 2022). Banana peel extract has been utilised for the consistent and green synthesis of AgNPs. The AgNPs resulting from the process have demonstrated good antimicrobial activity against pathogenic microorganisms (Bankar *et al.*, 2010; Ibrahim, 2015).

On the other hand, very little information is available on the banana flower, one of the secondary products of the banana plant, even though it is used widely as an important wild food and medicinal source (Sheng *et al.*, 2010; Padam *et al.*, 2014; Lau *et al.*, 2020; Hikal *et al.*, 2022). Recent studies have shown that banana flower contains several bioactive substances including polyphenols (phenolic acids and flavonoids), phytosterols, triterpenoids unsaturated fatty acids, saponins, polysaccharides, alkaloids, and tannins (Lau *et al.*, 2020). These phytochemicals possess diverse phytochemical properties such as antioxidation, antibacterial, anticancer, antidiabetic,

and anti-inflammatory action (Jamuna and Nandini, 2014; Sitthiya *et al.*, 2018). Experiments have shown that the polyphenolic compounds present in banana flowers could act as both reducing and capping agents for the synthesis of AgNPs (Stirbescu *et al.*, 2019). The preparation of AgNPs from banana flower extract can not only reduce the preparation cost, but also maximise the utilisation of agricultural resources. However, as a potential reducing and capping agent, the preparation of AgNPs from banana flower extract, and the exploration of the biological activity of formed AgNPs are very limited.

The present work thus aimed to synthesise AgNPs by a green biological route using an extract derived from banana flower, and explore their properties using UV-vis, FT-IR, TEM, XRD, TGA, and zeta potential analyses. In addition, the AgNPs were studied for their *in vitro* antibacterial activity, including the antibacterial mechanism responsible for their action.

Materials and methods

Materials and reagents

Silver nitrate (AgNO₃, AR), glutaraldehyde (25%), ethanol (100%), phosphate-buffered saline (PBS), and trypticase soy broth (TSB) were purchased from Macklin and HuanKai Microbial Company, China. Reactive oxygen detection kits were purchased from Beyotime Company, China.

Preparation of banana flower extract

Banana flowers were washed with distilled water, and dried at ambient temperature. The flowers (20 g) were put in 50 mL distilled water, and heated for 30 min at 60°C. After cooling to room temperature, the banana flower extract (BFE) was filtered and stored at 4°C for later use. The composition of BFE was analysed by liquid chromatography-mass spectrometry (LC-MS) (Q Exactive, American).

Synthesis of silver nanoparticles

The synthesis of the AgNPs was achieved following the method described in an earlier study with simple modifications (Alsammarrarie *et al.*, 2018). Briefly, 12 mL of 4 mM silver nitrate solution was mixed with 1 mL of 0.4 g/mL BFE, and stirred at 90°C for 120 min. The colour of solution turned reddish-brown which indicated that BFE-coated AgNPs were obtained. When the reaction was

complete, the AgNPs were centrifuged repeatedly at 12,000 rpm for 20 min in a centrifuge (Cence H1750R, China), and the precipitate was resuspended in distilled water. The concentration of the synthesised AgNPs was determined by ICP-MS (Thermo Fisher ICAP RQ, Germany), and they stored at 4°C for further investigation.

Characterisation of AgNPs

The FT-IR measurements of freeze-dried powder samples of the AgNPs and BFE were carried out using FT-IR spectrometer (Thermo Fisher IS50R, USA) using KBr pellets. The FT-IR spectra were recorded at a resolution of 1 cm⁻¹ in a range of 4000 - 400 cm⁻¹. The X-ray diffraction (XRD) patterns of powdered samples of the AgNPs in a 2θ range from 10° to 85° were carried out with an X-ray diffractometer (Rigaku SmartLab, Japan) using a Cu Kα radiation source with λ = 1.54178 Å, an operating voltage of 40 kV, and a current of 40 mA. For TEM characterisation, a drop of the synthesised AgNPs was placed onto a carbon-coated copper grid, and dried at ambient temperature before the morphology of the AgNPs was observed using TEM (Hitachi HT-7700, Japan). In addition, the average particle size of the AgNPs was measured with Image-J software. The thermal stability and associated weight loss of the AgNPs were evaluated by thermal gravimetric analysis (TGA NETZSCH, Germany) in a temperature range from 25 to 700°C, with a nitrogen flow rate of 20 mL/min at a heating rate of 10°C/min. The zeta potentials of the AgNPs were determined by laser light scattering spectrometer (Brookhaven BI-200SM, American). To determine the storage stability, the AgNPs in different fluids (water or ethanol) were placed in transparent glass bottles. The bottles were kept in the dark at room temperature for 7 d.

Antibacterial activity of the silver nanoparticles

The ATCC (American Type Culture Collection) provided the standard strains and codes for the studied strains. *Staphylococcus aureus* (ATCC29213) and *Escherichia coli* (ATCC8739) strains were obtained from Guangdong Institute of Microbiology, and used to characterise the antibacterial effects of the AgNPs. The growth curve was used to determine the antibacterial activity of the AgNPs. Briefly, bacterial strains were inoculated into nutrient agar medium, and the plates were incubated overnight in a shaking incubator (ZhiCheng ZWY-

100H, China) at 37°C at 200 rpm. Then the bacterial liquid was diluted with trypticase soy broth (TSB) medium to a concentration of 10⁶ CFU/mL. Next, 100 μL of different concentrations of the AgNPs were added sequentially to well plates, followed by 100 μL of TSB medium. There were three samples of each concentration. Finally, the well plate was incubated for 24 h in a growth curve analyser (OD Growth Curves Ab Ltd FP-1100-C, Finland), and measured at regular intervals. In all test, deionised water was used as the control.

Assay for cell membrane permeability

The antibacterial action of the AgNPs was assessed by examining evidence of leakage of intracellular proteins and nucleic acids from the bacteria by measuring the UV absorbance at 260 and 280 nm using a UV-vis spectrometer (Mepada UV-1800PC, China). Specifically, after incubating overnight, the *S. aureus* and *E. coli* were centrifuged at 10,000 rpm for 15 min, washed twice, and then resuspended with sterile PBS (pH = 7.2) to a cell concentration of ~10⁸ CFU/mL. The bacterial suspension mixed with concentrations of the AgNPs (0.5 and 1 × MIC) was incubated at 37°C for 4 h. Every hour, the bacterial suspension was centrifuged at 10,000 rpm for 15 min, and the optical density at 260 nm (OD₂₆₀) and 280 nm (OD₂₈₀) were determined. The bacterial suspension without the addition of the AgNPs was used as a control.

TEM characterisation of bacterial morphology

The characterisation of bacterial morphology with TEM used a method reported earlier with some modifications (Song *et al.*, 2019). The *S. aureus* and *E. coli* suspension mixed with the AgNPs was incubated at 37°C for 24 h. Next, the cell suspension was centrifuged at 10,000 rpm for 15 min, collected, and then resuspended with 2.5% glutaraldehyde at 4°C for 6 h. The bacterial cells were again collected by centrifuging at 10,000 rpm for 15 min, and washed with PBS (pH = 7.2) twice. The cell pellets were dehydrated by centrifugation with a sequential gradient of aqueous ethanol solutions (30, 50, 70, 80, 90, and 100%) for 15 min. Finally, the cells were resuspended in 100% ethanol.

The sample was placed onto a carbon-coated copper grid, and dried at ambient temperature, and the morphology of the bacteria was observed using TEM (Hitachi HT-7700, Japan).

Assay for ROS

Fluorescence microscopy for ROS detection

The ROS production was determined using a reactive oxygen detection kit (Beyotime S0033S, China). Bacterial suspension incubated overnight was washed with fresh TSB and resuspended to a cell concentration of $\sim 10^8$ CFU/mL. Next, 2,7-dichlorofluorescein diacetate (DCFH-DA) was added to the culture at a final concentration of 10 μ M, and incubated at 37°C for 30 min to load the probes. After loading, the culture was centrifuged and washed with PBS (pH = 7.2) twice to remove the excess unloaded probes, and the bacterial cells were treated with the AgNPs at the MIC concentration for 2 h. The result was observed using a fluorescence microscope (Olympus IX71, Japan).

Effect of antioxidants on antibacterial activity of AgNPs

The antioxidant N-acetyl-L-cysteine (NAC) was used to investigate the effect of ROS on the antibacterial activity of the AgNPs (Zafarullah *et al.*, 2003). To do this, the bacterial broth of *E. coli* or *S. aureus* was divided into two sets of cultures, with and without NAC. The AgNPs in each set were used as the treatment group, and those without the AgNPs were used as the control group. OD₆₀₀ values were measured periodically using a growth curve analyser (Oy Growth Curves Ab Ltd FP-1100-C, Finland).

Statistical analysis

Statistical analysis of all experimental data was carried out using Origin 2019b software, and results were expressed as mean \pm standard deviation (SD) of triplicate determinations ($n = 3$).

Results and discussion

Characterisation of banana flower extract and the synthesised silver nanoparticles

The UV-vis spectra of BFE and the AgNPs are shown in Figure 1a. For BFE, there were no absorption peaks in the wavelength range of 300 and 600 nm. The absorption peak for the AgNPs was at 412 nm, and the width at half height was narrow, which was consistent with the typical silver surface plasmon resonance (SPR), and in agreement with the results previously reported by Cheng *et al.* (2020). The AgNPs synthesised were brownish red in colour (see inset picture in Figure 1a), which was an indication of AgNO₃ reduction and colloidal silver

formation from BFE. Specifically, previous studies have shown that the natural reducing agent exhibited a strong complexation for silver ions, and can reduce them to silver, which appear brownish red (Ameen *et al.*, 2018). Table 1 lists the biomolecule groups in the aqueous extract of BFE which contains flavonoids, carbohydrates, alkaloids, free fatty acids, and saponins. In previous study, Mathew and Negi (2021) found that BFE contained phenolic substances such as rutin; meanwhile Nadumane (2014) confirmed that BFE contained carbohydrates, phenolics, proteins, and flavonoids which were consistent with our results. These bioactive substances may serve as bioreductants and stabilisers for the synthesis of AgNPs.

In order to further confirm the synthesis of the AgNPs, the infrared spectra of BFE alone and the AgNPs were obtained, and are shown in Figure 1b. The stretching vibration peak of the phenolic group (-OH) located at 3399 cm⁻¹, and the C-H in the methyl or methoxy group located at 2921 cm⁻¹ appeared in both BFE and the AgNPs, thus indicating that the phenol and methoxy groups did not change during the synthesis of the AgNPs. The phenolic and methoxy groups in plant extract play an important role in many properties such as antioxidation, anticancer, and free radical scavengers (Sheng *et al.*, 2014). Therefore, the AgNPs may still retain some of the biological activity of BFE. The nitrogen-hydrogen (N-H) stretching vibration peak of the amide bond of protein, and the carbon-oxygen (C-O) vibration peak in the ether group at 1615 and 1051 cm⁻¹ in BFE were red-shifted to 1622 and 1071 cm⁻¹ in the AgNPs. In addition, the C-H stretching vibration of alkanes at 1442 cm⁻¹ and the carbon oxygen (C-O) vibration peaks of carboxylic acid at 1311 cm⁻¹ disappeared in the AgNPs, but a new peak appeared at 1384 cm⁻¹. This strongly suggested that the silver was coordinated with the oxygen in a carbonyl structure of the BFE, and promoted functional groups of constituents of BFE such as flavonoids and saponins. In turn, these materials could adhere to the surface of the AgNPs and act in the dual role of a bioreductant and capping agent, thus preventing agglomeration thereby maintaining the dispersion and stability of the suspensions of the AgNPs (Ibrahim, 2015).

The XRD analysis was used to characterise the structure of crystalline materials (Figure 1c). The XRD pattern of the AgNPs exhibited five peaks at 38.20°, 44.20°, 64.56°, 77.84°, and 81.74° that were distinctive based on the standard data of silver in card

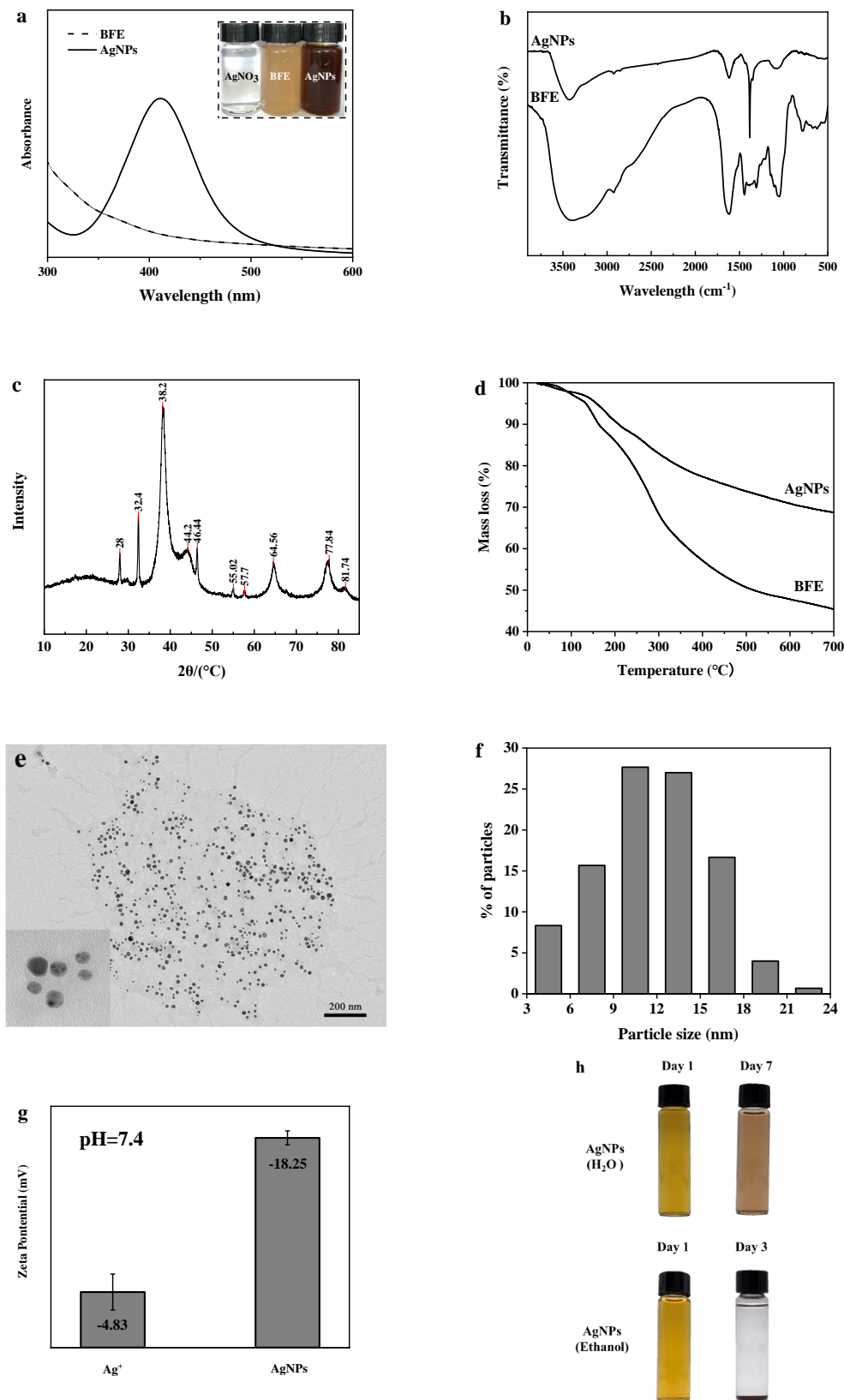


Figure 1. Characterisation of AgNPs. **(a)** UV-vis spectra, inset shows colour of BFE, AgNO₃, and the synthesised AgNPs; **(b)** FTIR spectra of BFE and AgNPs; **(c)** XRD pattern of AgNPs; **(d)** TGA analysis of BFE and AgNPs; **(e)** TEM images, inset is the high-resolution TEM image; **(f)** size distributions of AgNPs; **(g)** zeta potential of AgNPs; and **(h)** storage stability of AgNPs.

Table 1. Analysis of chemical composition of banana flower extract.

Name	Chemical Formula	Molecular Weight	Retention Time [min]
Trigonelline	C ₇ H ₇ NO ₂	137.04768	0.907
L-Isoleucine	C ₆ H ₁₃ NO ₂	131.09463	1.491
Citric acid	C ₆ H ₈ O ₇	192.027	1.062
Indole-3-acrylic acid	C ₁₁ H ₉ NO ₂	187.06333	4.532
Hexose	C ₆ H ₁₂ O ₆	180.06339	0.905
Guanosine	C ₁₀ H ₁₃ N ₅ O ₅	283.09167	1.259
Oleic acid	C ₁₈ H ₃₄ O ₂	282.25588	0.901
Byzantionoside B	C ₁₉ H ₃₂ O ₇	372.2148	24.147
Corchorifatty acid F	C ₁₈ H ₃₂ O ₅	328.22497	18.793
D (+)Glucose	C ₆ H ₁₂ O ₆	180.06339	0.84
Paederoside	C ₁₈ H ₂₂ O ₁₁ S	446.08828	14.062
NP-020521	C ₁₈ H ₃₂ O ₃	296.23514	22.107
Sinapoylglucose	C ₁₇ H ₂₂ O ₁₀	386.1213	10.998
Vanillin	C ₈ H ₈ O ₃	152.04734	10.367
Rutin	C ₂₇ H ₃₀ O ₁₆	610.15338	14.785
Maleic acid	C ₄ H ₄ O ₄	116.01096	1.254
5-OxoETE	C ₂₀ H ₃₀ O ₃	318.21949	22.107
12-oxo phytodienoic acid	C ₁₈ H ₂₈ O ₃	292.20384	21.557
D- α -hydroxyglutaric acid	C ₅ H ₈ O ₅	148.03717	1.082
NP-011548	C ₁₈ H ₃₄ O ₃	298.25079	22.493
Gentiopicrin	C ₁₆ H ₂₀ O ₉	356.11073	13.461
Glutaconic acid	C ₅ H ₆ O ₄	130.02661	1.275

U (Joint Committee on Powder Diffraction Standards (JCPDS), NO:04-0783). These peaks corresponded to reflection from (111), (200), (220), (311), and (222) crystal planes, thus indicating a face-centred cubic (FCC) structure of silver. In addition to these characteristic peaks of silver, a few unidentified crystalline peaks (marked with *) also appeared in the XRD pattern. These unidentified peaks might have been due to the crystallisation of the organics (polysaccharides and proteins) derived from BFE on the surface of the AgNPs (Rajivgandhi *et al.*, 2019). Similar results have been obtained for AgNPs biosynthesised using other plant extracts such as *Dillenia indica* bark and *Bauhinia variegata* flower (Mohanty and Jena, 2017; Johnson *et al.*, 2018).

The thermogravimetric analysis (TGA) was performed on the synthesised AgNPs. As shown in Figure 1d, the obvious decomposition of individual BFE began around 200°C, and the decomposition reached nearly 50% around 400°C. In contrast, the

decomposition for the AgNPs was only 70% at 700°C, thus indicating the good thermal stability of the AgNPs, which is possibly attributable to the thermal decomposition of the bioactive substances (capping agent) on the AgNPs surfaces.

A typical TEM micrograph of AgNPs is shown in Figure 1e. The synthesised AgNPs had a spherical shape, uniform morphology, and the size of the particle varied from 3 to 24 nm with an average size of 11.86 ± 3.88 nm (Figure 1f). The surface charges of the nanoparticles were determined by the zeta potential value, which describes the degree of stability of colloidal dispersion nanoparticles. A negative zeta potential of approximately -18.25 mV was recorded in the present work, thus suggesting higher stability of the synthesised AgNPs (Figure 1g). The greater negative surface charge potential value might be attributed to the effective functional constituents as capping agents present in the BFE extract. Furthermore, the stability of the AgNPs in

pure water and ethanol system was verified (Figure 1h). The AgNPs could well disperse in water and remain stable for seven days without precipitation. However, the AgNPs was stable in ethanol for only two days and precipitate at day 3, thus indicating that the AgNPs had different storage stability in different biological fluids.

These results confirmed that BFE had strong ability to reduce AgNO_3 to form stable colloidal silver. The use of other plant extracts has also been shown to be effective in producing AgNPs (Salayová *et al.*, 2021). In short, the results observed in the present work were consistent with reports from other researchers that support the use of plant extracts as good bioreductants and capping agents for the synthesis of AgNPs.

Antibacterial activity of silver nanoparticles

The effect of the AgNPs on the increase in OD_{600} , a measure of microbial growth, of *S. aureus* and *E. coli*, is shown in Figures 2a and 2b. As the concentration of the AgNPs increased, the growth of the two bacteria was significantly inhibited. When the AgNPs concentration was below $1.0 \times \text{MIC}$, the growth of the two bacteria was delayed to a certain extent but was not significantly inhibited. For concentrations of the AgNPs higher than $1.0 \times \text{MIC}$, OD_{600} values remained below 0.2 throughout the incubation, thus indicating that the growth of bacterial was obviously inhibited. While treatment with the AgNPs showed antibacterial effects against *S. aureus* and *E. coli*, treatment with BFE alone did not exhibit any antibacterial activity against the bacteria.

The MIC values of the AgNPs against *S. aureus* (Gram-positive) and *E. coli* (Gram-negative) were 32 and 16 $\mu\text{g/mL}$, respectively, which were consistent with previous studies (Padalia and Chanda, 2021). This could have been due to differences in their respective cell wall structures. However, our finding was in contrast to an earlier investigation by Paredes *et al.* (2014), who found Gram-positive to be more susceptible to the effect of AgNPs than Gram-negative, and to other studies that have reported comparable antibacterial effects for AgNPs against Gram-positive and Gram-negative bacteria (Du *et al.*, 2019). The present work observed lower MIC values against *S. aureus* and *E. coli* than values reported in some other studies (Du *et al.*, 2019; Devanesan and AlSalhi, 2021). This difference might have been due to the smaller particle size of the AgNPs synthesised in the present work.

The studies of antimicrobial activity of AgNPs are important because of their potential applications in cleaning and disinfecting practices in the food industry (Kanikireddy *et al.*, 2020). Concerns have been raised about the possible migration and cytotoxicity effects of AgNPs when used in such practical applications (Rezvani *et al.*, 2019). While laboratory studies have shown that these migrated Ag species in food are non-toxic to human cells at concentrations lower than 10 mg/L (AshaRani *et al.*, 2009), due to their small size and variable properties, the toxicological impact of these materials must be evaluated in practical food safety applications in order to determine their total effects in real world conditions, especially on food safety.

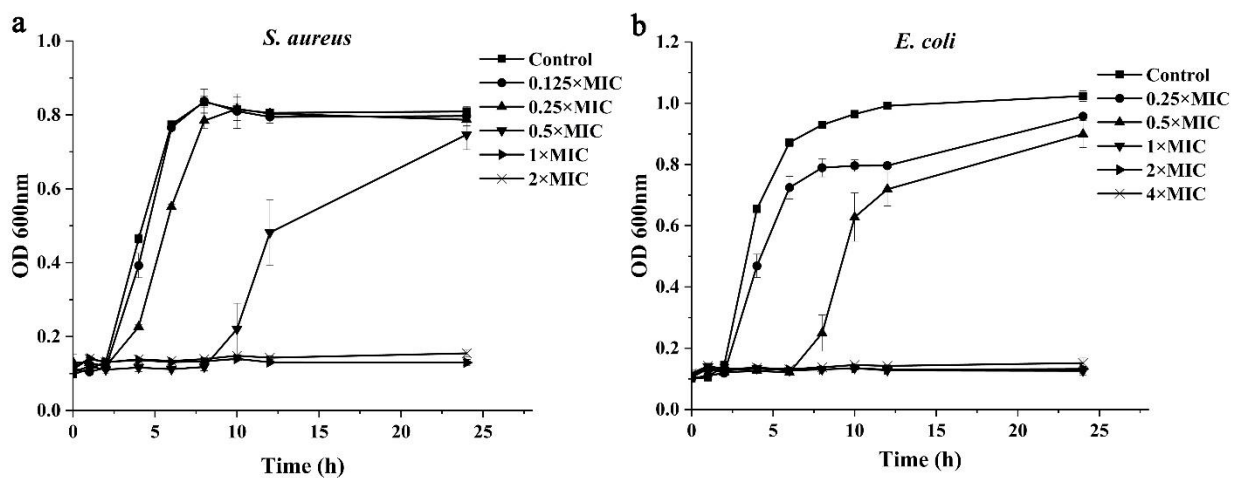


Figure 2. Effects of AgNPs concentration on the growth of *S. aureus* and *E. coli*. (a) OD growth curves of *S. aureus*; and (b) OD growth curves of *E. coli*. Controls were cells untreated with AgNPs.

Changes in membrane permeability

After treatment with the AgNPs, cell membrane permeability (as reflected in released cellular components) was measured by UV absorption (Figures 3a - 3d). The spectral peaks at 260 and 280 nm of the cell debris were generally attributed to the absorption of nucleic acids and macromolecular proteins (Saratale *et al.*, 2020).

Because of membrane permeability brought on by exposure to the AgNPs, there was significant increase in OD₂₆₀ in the cells treated with 1.0 × MIC of AgNPs, while there was a slight increase in OD₂₆₀ in cells treated with in 0.5 × MIC. This dose-related response indicated AgNP-related leakage of intracellular constituents, and was consistent with earlier work (Vazquez-Muñoz *et al.*, 2019).

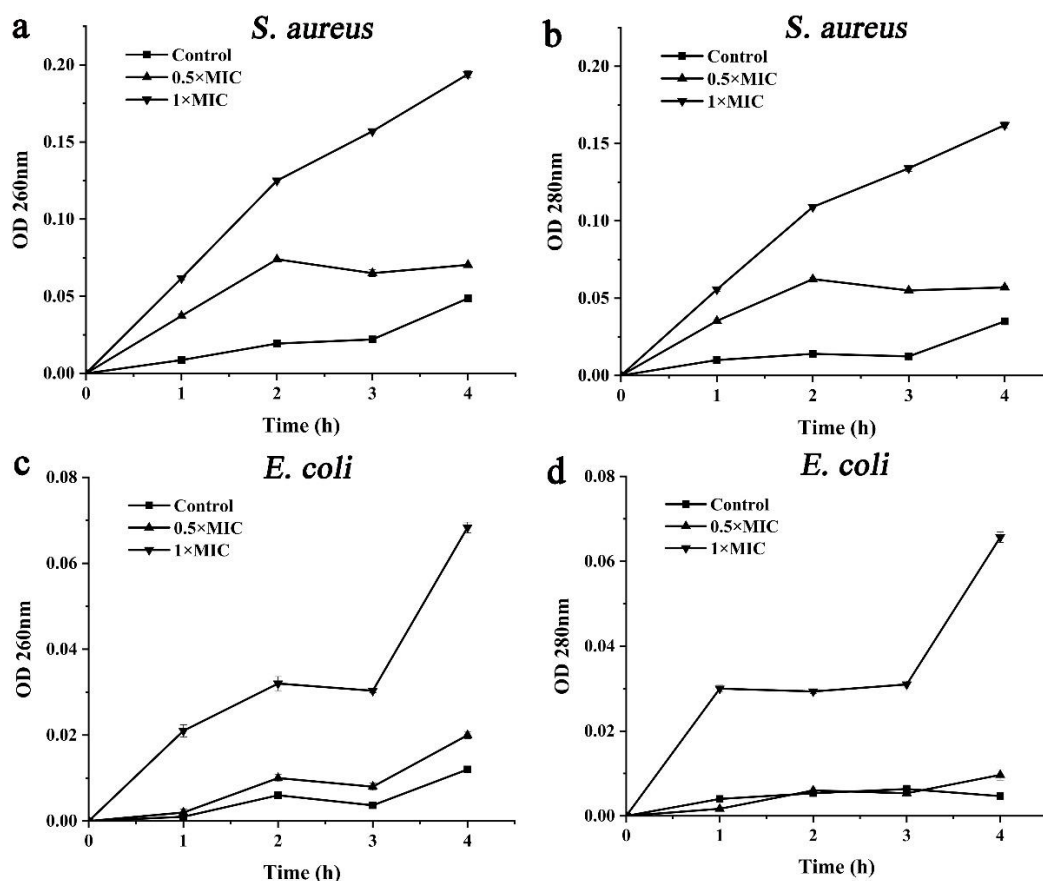


Figure 3. Effect of AgNPs concentration on cell membrane permeability. (a) absorbance of *S. aureus* at 260 nm; (b) absorbance of *S. aureus* at 280 nm; (c) absorbance of *E. coli* at 260 nm; and (d) absorbance of *E. coli* at 280 nm. Controls were cells untreated with AgNPs.

Changes in membrane morphology

The morphological changes of *S. aureus* and *E. coli* before or after treatment with AgNPs were observed with TEM (Figure 4). Untreated *S. aureus* and *E. coli* cells were structurally intact, and exhibited typical smooth and normal bacterial cell morphology (Figures 4a and 4b). After treatment with the AgNPs, the cell morphology of *S. aureus* and *E. coli* cells showed some obvious changes, *i.e.*, the cell membrane became rough and fuzzy, and some cells were collapsed, ruptured, and lost structural integrity (Figures 4c and 4d). This observation was consistent with the results of TEM morphological changes in the

cell walls of *S. aureus* or *E. coli* induced by exposure to AgNPs (Ahmad *et al.*, 2015; Baek *et al.*, 2017).

Direct contact of the AgNPs with bacterial cell walls has been suggested as an antibacterial mechanism instead of or in addition to some chemical toxicity (Li *et al.*, 2021). In this view, AgNPs cause irreparable damage to the cellular membrane which results in the accumulation of nanoparticles in the cytoplasm, thus leading to cell death.

Changes in ROS production

In addition to cell membrane damage, it is possible that the AgNPs might also exert their

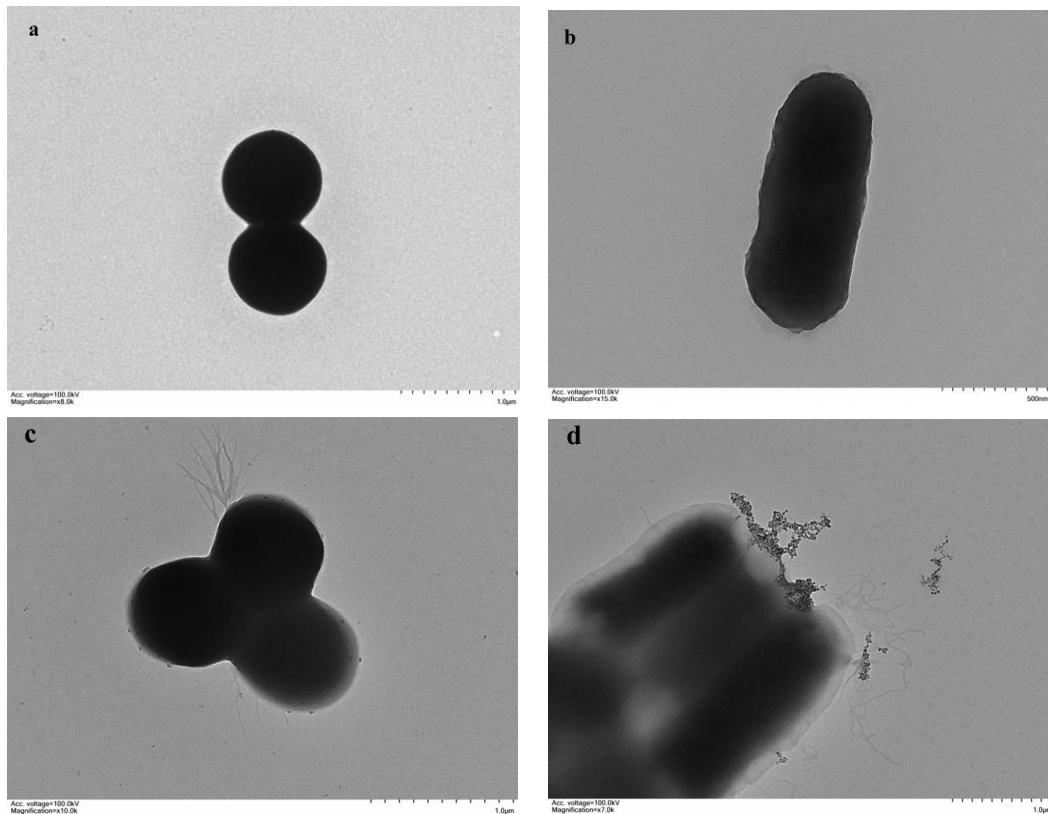


Figure 4. TEM images of bacterial cells incubated with AgNPs. (a) untreated cells of *S. aureus* and (b) untreated cells of *E. coli*; (c) cells of *S. aureus* treated with AgNPs; and (d) cells of *E. coli* treated with AgNPs.

antimicrobial effects through other means as well. It has been reported that the antibacterial mechanism of AgNPs may involve generation of ROS (reactive oxygen species) (Li *et al.*, 2021). Based on previous studies, the pathways for ROS induced by AgNPs can be summarised as follows: (1) in extracellular space, AgNPs can induce the generation of oxygen free radicals (O^{\bullet}) and superoxide free radicals ($O_2^{\bullet-}$) during the leaching process, which is considered as the important source of cell membrane disruption (Faiz *et al.*, 2018); (2) on the cell membrane, AgNPs are likely to induce the electrons of membrane-bound respiratory chain enzymes to leak into the cytoplasm, and react with cytoplasmic oxygen (O_2) to form superoxide radicals ($O_2^{\bullet-}$) (Gunawan *et al.*, 2020); (3) in the intracellular space, the formed superoxide radicals ($O_2^{\bullet-}$) can damage the Fe-S cluster to release the Fe^{2+} , which can participate in Fenton action to reduce hydroxyl radical (OH^{\bullet}). Consequently, the free radicals or ROS can cause conformational changes in membrane proteins and DNA structures, thus ultimately resulting in cell death (Gunawan *et al.*, 2020).

To test this hypothesis, the internal ROS generation with the AgNPs treatment was explored

using a DCFH-DA probe, which can be hydrolysed into 2,7-dichlorofluorescein (DCFH) in the cytoplasm and then oxidised into a fluorescent substance, 2,7-dichlorofluorescein (DCF), by ROS. The amount of green fluorescence is related to the level of ROS observed in fluorescence microscopy. As shown in Figures 5a and 5b, there is almost no fluorescence (*i.e.*, no ROS production) in untreated bacteria. In contrast, fluorescence was observed in the AgNP-treated cells, thus indicating the presence of ROS (Figures 5c and 5d) which was attributed as part of the bactericidal mechanism of AgNPs (Ahmad *et al.*, 2015).

To further confirm the involvement of ROS in the antibacterial mechanism of the AgNPs, bacterial growth in the presence of NAC was also measured. Previous experiments have demonstrated that the growth of bacteria was inhibited by the AgNPs at the MIC concentration, so the growth curves of both bacteria with the AgNPs at the MIC concentration were measured for 12 h. Figures 5e and 5f show that the death rate of the AgNPs was significantly decreased in the presence of NAC. Exposure to NAC by itself did not show any lethal effect on the bacteria. AgNPs alone showed strong antibacterial activity.

However, mortalities decreased when NAC was added to the AgNPs. These results showed that the antibacterial activity of the AgNPs was attenuated in

the presence of antioxidant. The same conclusion was also drawn in the experiments of Xu *et al.* (2012) and Song *et al.* (2019).

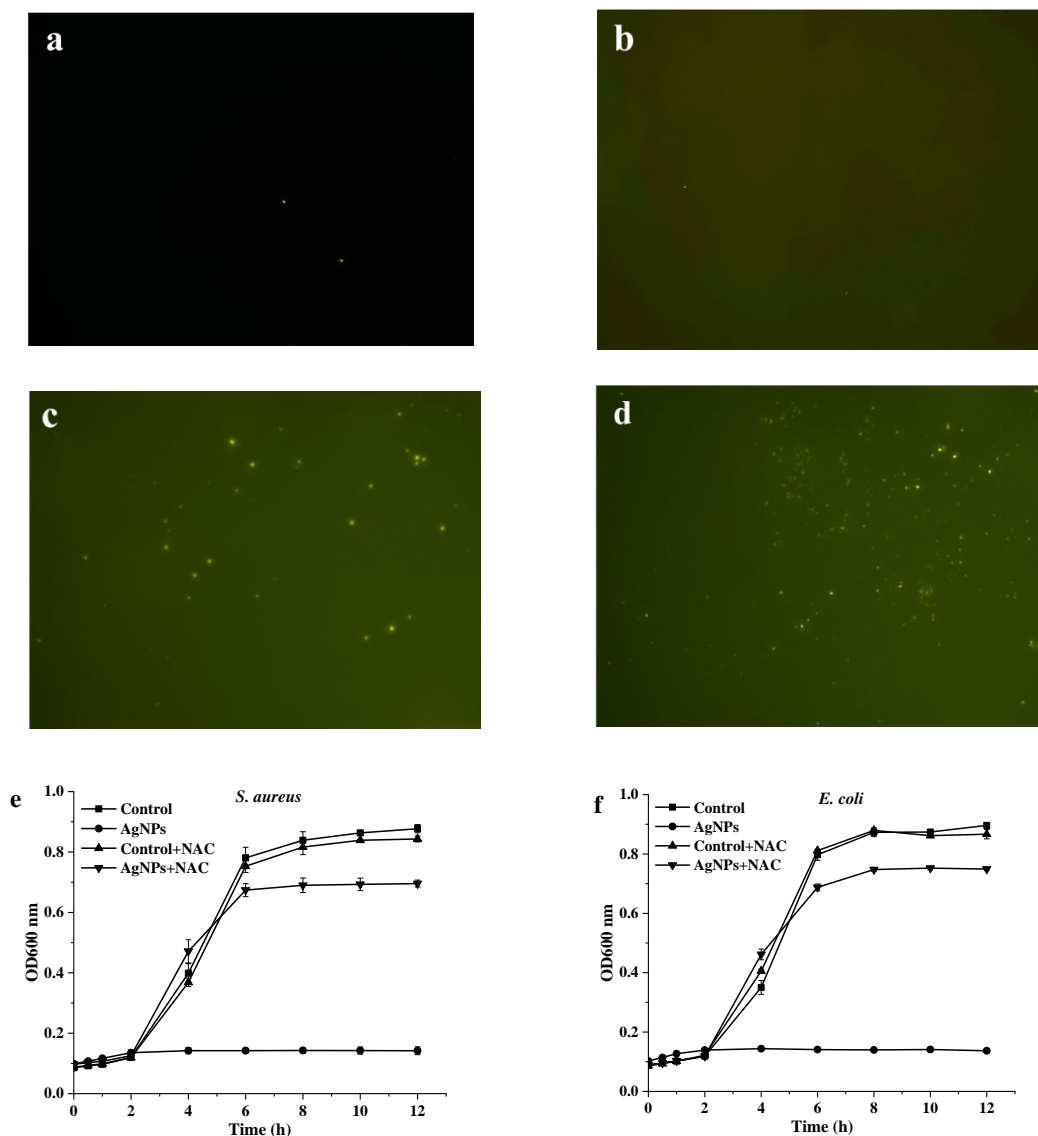


Figure 5. Detection of ROS generation with the AgNPs treatment. (a - d) Fluorescence microscope images of *S. aureus* (untreated), *E. coli* (untreated), *S. aureus* (treated with AgNPs), and *E. coli* (treated with AgNPs), respectively; (e - f) OD growth curves of *S. aureus* and *E. coli* in the presence of NAC and AgNPs.

Conclusion

In the present work, banana flower extract was used as both a bio-reductant and a capping agent for AgNPs biosynthesis. The synthesised AgNPs had spherical shape, uniform morphology, and good dispersion. They exhibited good *in vitro* antibacterial activity against *S. aureus* and *E. coli*, with MIC values of 32 and 16 $\mu\text{g/mL}$, respectively. Cell membrane damage and ROS induction were shown to be significant antibacterial factors in the antibacterial

mechanism. Further studies will be conducted on the use of AgNPs in actual food and food packaging for food quality control as a part of a comprehensive investigation of the use, migration, toxicology, and safety of AgNPs.

Acknowledgement

Professor Don and Karen Barnes are gratefully acknowledged for their kind assistance and revisions of English grammar and quality of this article.

References

- Ahmad, R., Mohsin, M., Ahmad, T. and Sardar, M. 2015. Alpha amylase assisted synthesis of TiO₂ nanoparticles: Structural characterization and application as antibacterial agents. *Journal of Hazardous Materials* 283: 171-177.
- Alsammarrarie, F. K., Wang, W., Zhou, P., Mustapha, A. and Lin, M. S. 2018. Green synthesis of silver nanoparticles using turmeric extracts and investigation of their antibacterial activities. *Colloids and Surfaces B - Biointerfaces* 171: 398-405.
- Ameen, F., AlYahya, S. A., Bakhrebah, M. A., Nassar, M. S. and Aljuraifani, A. 2018. Flavonoid dihydromyricetin-mediated silver nanoparticles as potential nanomedicine for biomedical treatment of infections caused by opportunistic fungal pathogens. *Research on Chemical Intermediates* 44(9): 5063-5073.
- Arce, V. B., Santillán, J. M. J., Muñetón Arboleda, D., Muraca, D., Scaffardi, L. B. and Schinca, D. C. 2017. Characterization and stability of silver nanoparticles in starch solution obtained by femtosecond laser ablation and salt reduction. *Journal of Physical Chemistry C* 121(19): 10501-10513.
- Arya, G., Kumari, R. M., Gupta, N., Kumar, A., Chandra, R. and Nimesh, S. 2018. Green synthesis of silver nanoparticles using *Prosopis juliflora* bark extract: Reaction optimization, antimicrobial and catalytic activities. *Artificial Cells Nanomedicine and Biotechnology* 46(5): 985-993.
- AshaRani, P. V., Mun, G. L. K., Hande, M. P. and Valiyaveetil, S. 2009. Cytotoxicity and genotoxicity of silver nanoparticles in human cells. *ACS Nano* 3(2): 279-290.
- Baek, S., Joo, S. H., Kumar, N. and Toborek, M. 2017. Antibacterial effect and toxicity pathways of industrial and sunscreen ZnO nanoparticles on *Escherichia coli*. *Journal of Environmental Chemical Engineering* 5(3): 3024-3032.
- Bankar, A., Joshi, B., Kumar, A. R. and Zinjarde, S. 2010. Banana peel extract mediated novel route for the synthesis of silver nanoparticles. *Colloids and Surfaces A - Physicochemical and Engineering Aspects* 368(1-3): 58-63.
- Cheng, T. H., Yang, Z. Y., Tang, R. C. and Zhai, A. D. 2020. Functionalization of silk by silver nanoparticles synthesized using the aqueous extract from tea stem waste. *Journal of Materials Science and Technology* 9(3): 4538-4549.
- Devanesan, S. and AlSalhi, M. S. 2021. Green synthesis of silver nanoparticles using the flower extract of *Abelmoschus esculentus* for cytotoxicity and antimicrobial studies. *International Journal of Nanomedicine* 16: 3343-3356.
- Du, J., Hu, Z. Y., Yu, Z. Y., Li, H. L., Pan, J., Zhao, D. B. and Bai, Y. H. 2019. Antibacterial activity of a novel *Forsythia suspensa* fruit mediated green silver nanoparticles against food-borne pathogens and mechanisms investigation. *Materials Science and Engineering C* 102(136): 247-253.
- El-Kheshen, A. A. and El-Rab, S. F. G. 2012. Effect of reducing and protecting agents on size of silver nanoparticles and their anti-bacterial activity. *Der Pharma Chemica* 4(1): 53-65.
- Faiz, M. B., Amal, R., Marquis, C. P., Harry, E. J., Sotiriou, G. A., Rice, S. A. and Gunawan, C. 2018. Nanosilver and the microbiological activity of the particulate solids versus the leached soluble silver. *Nanotoxicology* 12(3): 263-273.
- Gunawan, C., Faiz, M. B., Mann, R., Ting, S. R. S., Sotiriou, G. A., Marquis, C. P. and Amal, R. 2020. Nanosilver targets the bacterial cell envelope: The link with generation of reactive oxygen radicals. *ACS Applied Materials and Interfaces* 12(5): 5557-5568.
- Guo, Z. C., Chen, Y., Wang, Y. H., Jiang, H. and Wang, X. M. 2020. Advances and challenges in metallic nanomaterial synthesis and antibacterial applications. *Journal of Materials Chemistry B* 8: 4764-4777.
- Hikal, W. M., Ahl, H. A. H. S., Bratovcic, A., Tkachenko, K. G., Sharifi-Rad, J., Kačaniová, M., ... and Atanassova, M. 2022. Banana peels: A waste treasure for human being. *Evidence-Based Complementary and Alternative Medicine* 2022: 7616452.
- Ibrahim, H. M. M. 2015. Green synthesis and characterization of silver nanoparticles using banana peel extract and their antimicrobial activity against representative microorganisms. *Journal of Radiation Research and Applied Sciences* 8(3): 265-275.

- Jamuna, J. B. and Nandini, C. D. 2014. Feeding of banana flower and pseudostem to diabetic rats results in modulation of renal GLUTs, TGF β , PKC and extracellular matrix components. *Nutrition, Metabolism and Cardiovascular Diseases* 24(6): 623-631.
- Johnson, P., Krishnan, V., Loganathan, C., Govindhan, K., Raji, V., Sakayanathan, P., ... and Palvannan, T. 2018. Rapid biosynthesis of *Bauhinia variegata* flower extract-mediated silver nanoparticles: An effective antioxidant scavenger and α -amylase inhibitor. *Artificial Cells Nanomedicine and Biotechnology* 46(7): 1488-1494.
- Joshi, A. S., Singh, P. and Mijakovic, I. 2020. Interactions of gold and silver nanoparticles with bacterial biofilms: Molecular interactions behind inhibition and resistance. *International Journal of Molecular Sciences* 21(20): 7658.
- Kanikireddy, V., Varaprasad, K., Rani, M. S., Venkataswamy, P., Reddy, B. J. M. and Vithal, M. 2020. Biosynthesis of CMC-guar gum-Ag0 nanocomposites for inactivation of food pathogenic microbes and its effect on the shelf life of strawberries. *Carbohydrate Polymers* 116053: 116053.
- Küp, Ö. F., Çoşkunçay, S. and Duman, F. 2020. Biosynthesis of silver nanoparticles using leaf extract of *Aesculus hippocastanum* (horse chestnut): Evaluation of their antibacterial, antioxidant and drug release system activities. *Materials Science and Engineering C* 107: 110207.
- Lau, B. F., Kong, K. W., Leong, K. H., Sun, J., He, X. M., Wang, Z. X., ... and Ismail, A. 2020. Banana inflorescence: Its bio-prospects as an ingredient for functional foods. *Trends in Food Science and Technology* 97: 14-28.
- Li, Z., Ali, I., Qiu, J., Zhao, H. Z., Ma, W. Y., Bai, A. Y., ... and Li, J. C. 2021. Eco-friendly and facile synthesis of antioxidant, antibacterial and anticancer dihydromyricetin-mediated silver nanoparticles. *International Journal of Nanomedicine* 16: 481-492.
- Liu, Y., Shi, L. Q., Su, L. Z., van der Mei, H. C., Jutte, P. C., Ren, Y. J. and Busscher, H. J. 2019. Nanotechnology-based antimicrobials and delivery systems for biofilm-infection control. *Chemical Society Reviews* 48: 428-446.
- Mathew, N. S. and Negi, P. S. 2021. Phenolic content and anti-oxidative attributes of various parts of wild banana (*Ensete superbum* Roxb. Cheesman) plant. *Journal of Food Biochemistry* 45(4): e13657.
- Mohanty, A. S. and Jena, B. S. 2017. Innate catalytic and free radical scavenging activities of silver nanoparticles synthesized using *Dillenia indica* bark extract. *Journal of Colloid and Interface Science* 496: 513-521.
- Nadumane, V. K. 2014. Anti-cancer potential of banana flower extract: An *in vitro* study. *Bangladesh Journal of Pharmacology* 9(4): 628-635.
- Nguyen, T. M. T., Huynh, T. T. T., Dang, C. H., Mai, D. T., Nguyen, T. T. N., Nguyen, D. T., ... and Nguyen, T. D. 2020. Novel biogenic silver nanoparticles used for antibacterial effect and catalytic degradation of contaminants. *Research on Chemical Intermediates* 46(3): 1975-1990.
- Osonga, F. J., Akgul, A., Yazgan, I., Akgul, A., Eshun, G. B., Sakhaee, L. and Sadik, O. A. 2020. Size and shape-dependent antimicrobial activities of silver and gold nanoparticles: A model study as potential fungicides. *Molecules* 25(11): 2682.
- Padalia, H. and Chanda, S. 2021. Synthesis of silver nanoparticles using *Ziziphus nummularia* leaf extract and evaluation of their antimicrobial, antioxidant, cytotoxic and genotoxic potential (4-in-1 system). *Artificial Cells Nanomedicine and Biotechnology* 49(1): 354-366.
- Paredes, D., Ortiz, C. and Torres, R. 2014. Synthesis, characterization, and evaluation of antibacterial effect of Ag nanoparticles against *Escherichia coli* O157: H7 and methicillin-resistant *Staphylococcus aureus* (MRSA). *International Journal of Nanomedicine* 9(1): 1717-1729.
- Padam, B. S., Tin, H. S., Chye, F. Y. and Abdullah, M. I. 2014. Banana by-products: An under-utilized renewable food biomass with great potential. *Journal of Food Science and Technology* 51(12): 3527-3545.
- Rajeshkumar, S. and Bharath, L. V. 2017. Mechanism of plant-mediated synthesis of silver nanoparticles - A review on biomolecules involved, characterisation and antibacterial activity. *Chemico-Biological Interactions* 273: 219-227.
- Rajivgandhi, G., Maruthupandy, M., Muneeswaran, T., Muneeswaran, T., Anand, M., Quero, F., ...

- and Li, W. J. 2019. Biosynthesized silver nanoparticles for inhibition of antibacterial resistance and biofilm formation of methicillin-resistant coagulase negative *Staphylococci*. *Bioorganic Chemistry* 89: 103008.
- Rezvani, E., Rafferty, A., McGuinness, C. and Kennedy, J. 2019. Adverse effects of nanosilver on human health and the environment. *Acta Biomaterialia* 94: 145-159.
- Salayová, A., Bedlovicová, Z., Daneu, N., Baláž, M., Lukáčová Bujnáková, Z., Balážová, L. and Tkáčiková, L. 2021. Green synthesis of silver nanoparticles with antibacterial activity using various medicinal plant extracts: Morphology and antibacterial efficacy. *Nanomaterials* 11: 1005-1025.
- Saratale, G. D., Saratale, R. G., Kim, D. S., Kim, D. Y. and Shin, H. S. 2020. Exploiting fruit waste grape pomace for silver nanoparticles synthesis, assessing their antioxidant, antidiabetic potential and antibacterial activity against human pathogens: A novel approach. *Nanomaterial* 10(8): 1457.
- Sheng, Z. W., Ma, W. H., Jin, Z. Q., Bi, Y., Sun, Z. G., Dou, H. T., ... and Han, L. N. 2010. Investigation of dietary fiber, protein, vitamin E and other nutritional compounds of banana flower of two cultivars grown in China. *African Journal of Biotechnology* 9(25): 3888-3895.
- Sheng, Z. W., Dai, H. F., Pan, S. Y., Wang, H., Hu, Y. Y. and Ma, W. H. 2014. Isolation and characterization of an α -glucosidase inhibitor from *Musa* spp. (Baxijiao) flowers. *Molecular* 19(7): 10563-10573.
- Sitthiya, K., Devkota, L., Sadiq, M. B. and Anal, A. K. 2018. Extraction and characterization of proteins from banana (*Musa sapientum* L) flower and evaluation of antimicrobial activities. *Journal of Food Science and Technology* 55(2): 658-666.
- Song, Z. Y., Wu, Y., Wang, H. J. and Han, H. Y. 2019. Synergistic antibacterial effects of curcumin modified silver nanoparticles through ROS-mediated pathways. *Materials Science and Engineering C* 99: 255-263.
- Soto, K. M., Quezada-Cervantes, C. T., Hernández-Iturriaga, M., Luna-Bárcenas, G., Vazquez-Duhalt, R. and Mendoza, S. 2019. Fruit peels waste for the green synthesis of silver nanoparticles with antimicrobial activity against foodborne pathogens. *LWT - Food Science and Technology* 103: 293-300.
- Stirbescu, N. M., Ion, R. M., Teodorescu, S., Olteanu, L., Dulama, I. D., Bucurica, I. A. and Stirbescu, R. M. 2019. Banana flower nectar - Mediated synthesis of silver nanoparticles. *Bulletin of the Transilvania University of Braşov Engineering Sciences - Series I* 12(2): 55-64.
- Vazquez-Muñoz, R., Meza-Villezcás, A., Fournier, P. G. J., Soria-Castro, E., Juarez-Moreno, K., Gallego-Hernandez, A. L., ... and Huerta-Saquero, A. 2019. Enhancement of antibiotics antimicrobial activity due to the silver nanoparticles impact on the cell membrane. *PLoS One* 14(11): e0224904.
- Xu, H. Y., Qu, F., Xu, H., Lai, W. H., Wang, Y. A. and Aguilar, Z. P. 2012. Role of reactive oxygen species in the antibacterial mechanism of silver nanoparticles on *Escherichia coli* O157:H7. *Biometals* 25(1): 45-53.
- Zafarullah, M., Li, W. Q., Sylvester, J. and Ahmad, M. 2003. Molecular mechanisms of N-acetylcysteine actions. *Cellular and Molecular Life Sciences* 60: 6-20.